Inorganic nanowires: a perspective about their role in energy conversion and storage applications

2011 J. Phys. D: Appl. Phys. 44 174032

(http://iopscience.iop.org/0022-3727/44/17/174032)

IOP PUBLISHING JOURNAL OF PHYSICS D: APPLIED PHYSICS

J. Phys. D: Appl. Phys. **44** (2011) 174032 (9pp) doi:10.1088/0022-3727/44/17/174032

Inorganic nanowires: a perspective about their role in energy conversion and storage applications

M K Sunkara, C Pendyala, D Cummins, P Meduri, J Jasinski, V Kumar, H B Russell, E L Clark and J H Kim

Department of Chemical Engineering and Conn Center for Renewable Energy Research, University of Louisville, Louisville, KY 40292, USA

E-mail: Mahendra@louisville.edu

Received 10 November 2010, in final form 23 December 2010
Published 14 April 2011
Online at stacks.iop.org/JPhysD/44/174032

Abstract

There has been tremendous interest and progress with synthesis of inorganic nanowires (NWs). However, much of the progress only resulted in NWs with diameters much greater than their respective quantum confinement scales, i.e. 10–100 nm. Even at this scale, NW-based materials offer enhanced charge transport and smaller diffusion length scales for improved performance with various electrochemical and photoelectrochemical energy conversion and storage applications. In this paper, these improvements are illustrated with specific results on enhanced charge transport with tin oxide NWs in dye sensitized solar cells, higher capacity retention with molybdenum oxide (MoO_3) NW arrays and enhanced photoactivity with hematite NW arrays compared with their nanoparticle (NP) or thin film format counterparts. In addition, the NWs or one-dimensional crystalline materials with diameters less than 100 nm provide a useful platform for creating new materials either as substrates for heteroepitaxy or through the phase transformation with reaction. Specific results with single crystal phase transformation of hematite (a-Fe_2O_3) to pyrite (FeS_2) NWs and heteroepitaxy of indium-rich InGaN alloy over GaN NW substrates are presented to illustrate the viability of using NWs for creating new materials. In terms of energy applications, it is essential to have a method for continuous manufacturing of vertical NW arrays over large areas. In this regard, a simple plasma-based technique is discussed that potentially could be scaled up for roll-to-roll processing of NW arrays.

(Some figures in this article are in colour only in the electronic version)

1. Introduction

Nanowires (NWs) are one-dimensional (1D) materials with diameters ranging from 1 to 100 nm and lengths of several micrometres or more. Interest in NWs originated from the curiosity to study and explore the quantum confinement effects in 1D materials. Under quantum confinement, the electronic, optical, magnetic and thermoelectric properties are expected to be different, which may lead to new applications [1]. However, very few studies resulted in the synthesis of NWs with diameters less than 10 nm and, of those, only some observed quantum confinement effects for NWs [2]. In spite of this, there has been significant interest in the synthesis of NWs with diameters from 10 to 100 nm as seen from the exponential increase in the number of papers published every year on the topic in the last decade [3]. The premise of this discussion is to show that NWs with diameters in tens of nanometres (nanoscale, but not in the quantum confinement region) are promising for a variety of applications by virtue of the 1D architecture and the expected crystallinity. Notwithstanding the obstacles with nanoscale device integration, NWs have actually been shown to have enhanced properties compared with bulk materials or thin films and, in some cases, nanoparticles.

In many electrochemical and photoelectrochemical energy conversion and storage applications, NW arrays and NW-based thin films represent unique opportunities due to their crystallinity and access to diameter length scale. Figure 1

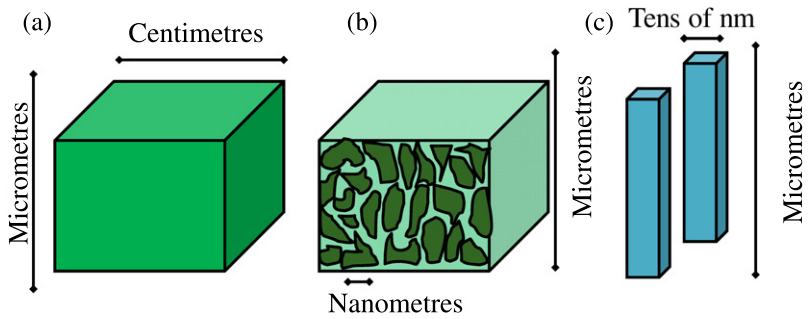

Figure 1. Schematics illustrating various length scales involved for charge transport with different film formats: (*a*) single crystalline film, (*b*) polycrystalline film and (*c*) NWs.

shows the schematic comparison of the size scale and its implications on the charge transport in single crystalline thin films, polycrystalline thin films and NW architectures. The difference between single crystalline and polycrystalline films is the presence of crystal grain boundaries that act as trap sites for the charge carriers and increase recombination losses, which drastically reduces device performance. NW architectures, shown in figure 1(*c*), provide high surface-to-volume ratios and also allow for controlling surface faceting and surface crystallinity for selectivity, catalysis and improved surface charge transport. The small diameters also offer a smaller length scale for diffusion of lithium ions and reacting species. Single crystalline thin films provide a 3D pathway for the movement of the charge carriers, either generated within or injected, and if the length needed to reach the contact or participate in a reaction is larger than the diffusion length, which is usually the case for bulk material systems, and thus recombination losses become significant. In addition, large single crystalline films of pristine quality are difficult to synthesize and in most cases have defects or dislocations that act as trap sites and increase recombination losses. In contrast, apart from having fewer or no defects, single crystalline NWs provide a direct pathway for charge transport, thus reducing the losses due to recombination. Deriving from the architecture in figure 1(*c*), efficient carrier generation can be achieved via NWs with lengths in the same size range as the absorption length. Increasing the length is analogous to increasing the film thickness, but without the problems of increased recombination.

In this paper, the role of NWs and their properties within the context of various electrochemical (lithium-ion batteries) and photoelectrochemical applications (dye sensitized solar cells and photoelectrochemical water splitting devices) are discussed. NWs can act as either single crystalline substrates or 1D hosts for creating new materials with control on size and crystallinity. Finally, a simple plasma-based process for producing NW arrays, their modification and their scale-up towards a roll-to-roll process is given in detail.

2. Role of 1D NWs in photoelectrochemical applications

2.1. Photoelectrochemical solar chemicals

Semiconductors, especially metal oxides and nitrides, are being studied extensively as photoactive materials for photoelectrochemical water splitting. The photoactive material should absorb sunlight efficiently (band gap in the 1.7–2.2 eV range), generate and separate charge carriers effectively, and have conduction and valence bands that straddle H_2/O_2 redox potentials to spontaneously drive water-splitting reactions [4]. Most of the materials satisfy these criteria partially, which limits their applications. With a band gap of 2 eV, iron oxide has the right band edge positions and is inexpensive, which should make it a suitable material [5]. However, iron oxide has been shown to be a mott insulator, i.e. it has very low charge carrier conductivity with diffusion length scales on the order of few nanometres [6a, 6b]. Typically, iron oxide thin films have been shown to exhibit no photoactivity due to little or no conductivity. The (0 0 1) plane of iron oxide has been shown to be 4 orders of magnitude more conductive than the [0 0 1] direction, but the large number of grain boundaries in polycrystalline films hinders this effect as well as causing high recombination rates and unordered oxygen vacancy planes [7]. Thus, the iron oxide is considered to be impractical for water-splitting applications. Recently, several attempts have been made to modify the conductivity of iron oxide by doping it with other elements, such as silicon, into nanometre scale particles [8]. Here, the NW array-based architectures offer interesting possibilities, i.e. the diameters offer smaller length scales for diffusion of minority carriers to the surface for electrochemical reactions and single crystallinity along the length scale offers appreciable conductivity for majority carriers. The length scales offer thicknesses necessary for absorbing solar radiation for generating electron–hole pairs. This is illustrated in a schematic in figure 2(*a*). Photoelectrochemical measurements were performed in a 3-electrode setup in a 1M potassium hydroxide (KOH) solution using the hematite NW array as the working electrode, platinum as the counter electrode and an Ag/AgCl reference electrode. The as-synthesized hematite NW arrays are n-type due to oxygen deficiency. In our experiments, under illumination, the hematite NW array electrode acts as photoanode evolving oxygen. Hydrogen is evolved at the platinum counter electrode. As shown in the data in figure 2(*c*), the as-synthesized NW arrays on iron foils exhibited appreciable photoactivity under visible light in comparison with thin films. The observed photoactivity was found to be reproducible with samples grown using a plasma oxidation scheme compared with that using thermal oxidation or other methods [9]. The observed photoactivity

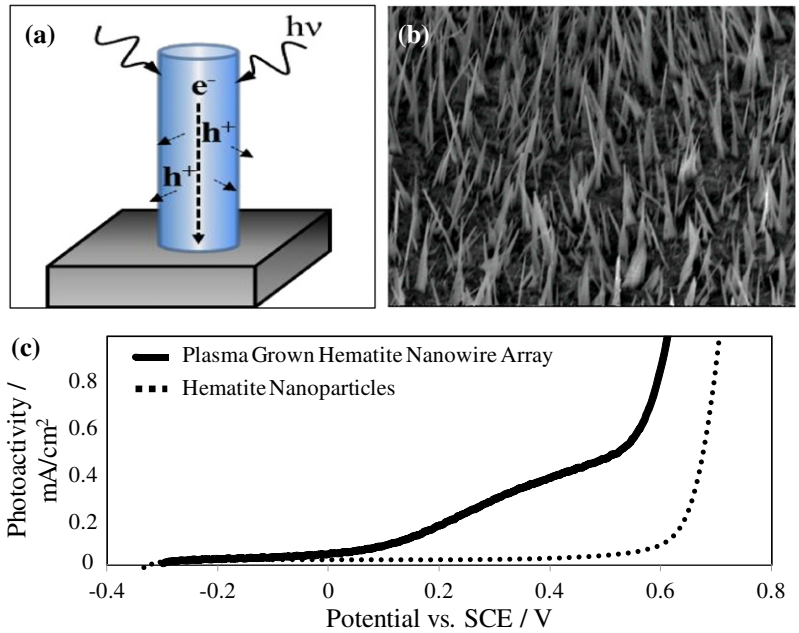

Figure 2. The use of NW array architectures for photoelectrochemical conversion of solar energy to fuels: (*a*) a schematic illustrating transport length scales for photogenerated carriers in NWs, (*b*) HRTEM image of as-synthesized, α-Fe_2O_3 NW array, (*c*) photoelectrochemical activity of as-synthesized α-Fe_2O_3 NW arrays grown on iron foils compared with nanocrystalline, α-Fe_2O_3 thin films.

was attributed primarily to a thin interfacial layer contact between the back contact and the NW array as well as enhanced conductivity along highly ordered oxygen vacancy planes in the (0 0 1) direction, which are perpendicular to the back contact of plasma-grown hematite NW arrays [9]. Thus, NW arrays compared with thin films should be an interesting format while determining the photoelectrochemical activity of unknown materials.

2.2. Photoelectrochemical solar electricity

In dye-sensitized solar cells, visible light-absorbing dye is adsorbed on a high surface area, wide band gap semiconductor NP network [10]. The excited electrons from highest occupied molecular orbital energy (HOMO) levels of the dye molecules are transferred to the conduction band of wide band gap semiconductor particles due to differences in work functions of the dye and semiconductors. This injection process is expected to be fast with time scales on the order of few hundred femtoseconds [11–13]. However, the diffusion of conduction band electrons through the NP network to the back contact can be on the order of few to tens of milliseconds [14]. In this regard, the NW-based films and architectures are expected to provide improved charge transport properties due to single crystallinity, as illustrated in the schematic in figure 3. In this case, the diffusion of electrons is expected to take place primarily on surfaces through trapping and de-trapping from surface states with energies located within a few tens of millielectronvolts below the conduction band. The density of such states depends highly on the surface ordering (or crystallinity). However, the transport characteristics of 1D structures for a variety of material systems have not yet been completely understood. Only recently has it been shown that titania NWs have faster charge transport than NPs [15] but

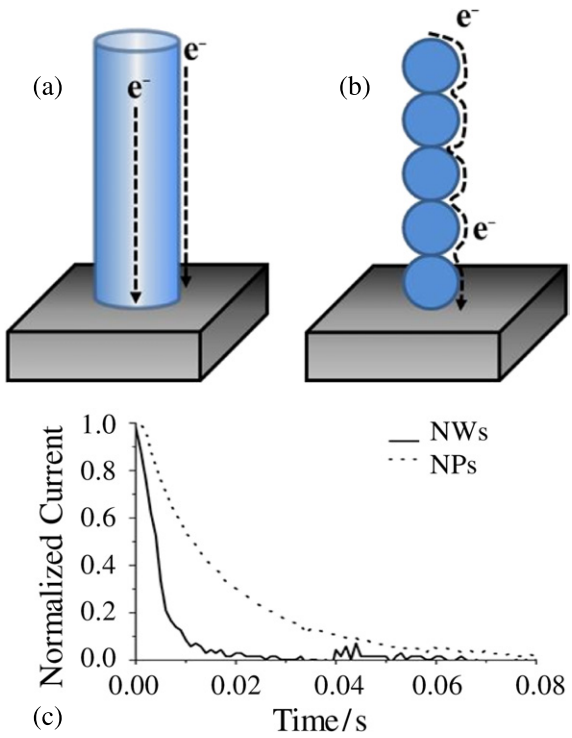

Figure 3. The use of NWs in dye sensitized solar cells: (*a*) and (*b*) schematics comparing the charge transport pathways for injected photogenerated carriers from adsorbed dyes between NWs and NP thin films and (*c*) the photocurrent decay data for dye sensitized solar cells made using SnO_2 NWs and NP thin films indicating faster current transport timescales in NW thin films.

only under low bias conditions, which limits their efficiency when using NW-based systems. On the other hand, zinc oxide NWs have been shown to have faster charge transport compared with NPs, but this material is not feasible for solar

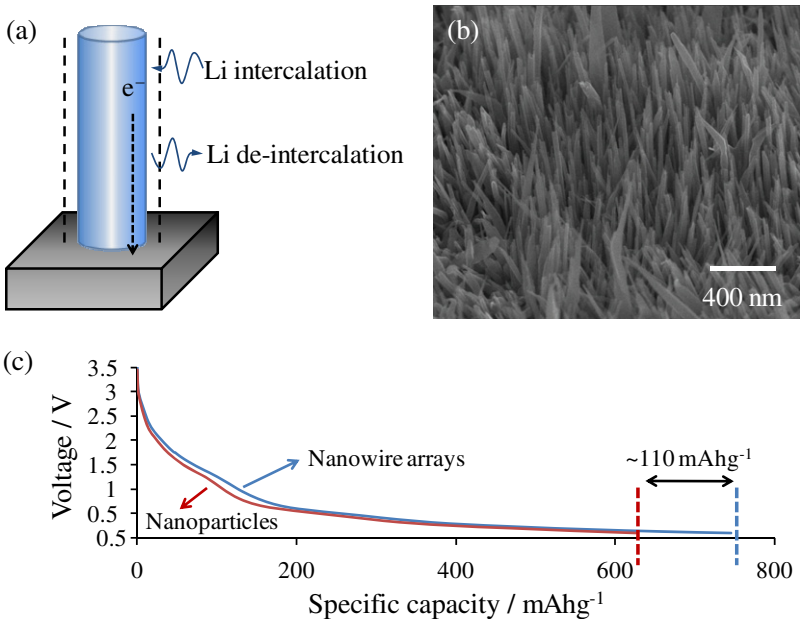

Figure 4. The use of NWs in lithium-ion battery applications: (*a*) schematic illustrating 1D electron conduction and low Li ion diffusion lengths in a NW array, (*b*) SEM image showing MoO_3 array grown directly on a steel substrate and (*c*) specific capacity performance during the first cycle of NW arrays and NPs indicating superior capacity retention with NW arrays.

cells. Therefore, it is clear that there are very few studies that show consistently faster transport in NWs than NPs for materials that are useful in solar cells. Our recent work showed that tin oxide NWs exhibits an order of magnitude improvement in the transport time scales within dye sensitized solar cells compared with that using NPs [16]. The transient photocurrent decay data shown in figure 3(*c*) illustrates faster charge transport in tin oxide NW-based thin films compared with NP-based films. In addition to transport properties, the recombination time scales are also important for improving the solar electricity energy conversion within dye sensitized solar cells. In the case of tin oxide NWs, the recombination properties are even 2 orders of magnitude better compared with their NP counterparts [17]. This opens up an interesting avenue for engineering the transport and recombination properties of materials such as titania NPs using tin oxide NWs and possibly allowing the use of other redox couples. In addition, the single crystalline NW format with controlled surface faceting offers interesting possibilities in terms of studying and exploiting fundamental surface transport properties.

3. Role of NWs in lithium-ion batteries and electrochromics

Lithium intercalation and deintercalation are important for two major applications: lithium-ion batteries and electrochromics. In both cases, it is important for the electrode materials to support bulk charge transport during lithium intercalation and deintercalation processes. In the case of lithium-ion batteries, high capacity, durability and rate performance pose some stringent requirements for satisfactory types of materials and designs. For electrochromics, fast intercalation and deintercalation into some selected set of material systems represent fast time scales for colour change and absorption properties. NW-based materials and architectures with diameters on the order of a few to tens of nanometres could be interesting for a variety of reasons: (a) fast intercalation/deintercalation time scales due to nanometre scale diameters, (b) complete lithiation and de-lithiation for high capacity retention and (c) better stress accommodation for mechanical durability [18, 19]. This is schematically illustrated in figure 4(*a*).

The biggest challenge for anodes in lithium-ion batteries is the inability to use high capacity materials such as silicon and tin due to mechanical degradation from expected, large volume expansions (400% and 250%, respectively). It has been shown that Si NW arrays on stainless-steel substrates sustain 80% of their theoretical capacity after 10 cycles [20]. Similarly, Ge NWs were also shown to retain capacities slightly lower than 1000 mAh g^{-1} until 20 cycles [21]. Reports have shown that $Sn_{78}Ge_{22}$/carbon core–shell NWs retain capacities as high as ~950 mAh g^{-1} after 45 cycles [22]. The increased capacity in these reports has been attributed to the increased surface area due to the NW architecture, reduced lithium-ion diffusion lengths from low NW diameters and better inherent strain relaxation properties of NWs. In the case of tin, it is easier to synthesize NWs in oxide form, i.e. tin oxide. However, for metal oxides, chemical degradation occurs to reduce the electrical conductivity for irreversible capacity loss.

In the case of metal oxides, a simple, generic concept involving metal nanocluster-covered metal oxide NWs was demonstrated for improving durability with high capacity retention using tin nanocluster-covered tin oxide NWs as the specific material system. In particular, the design consists of decorating the SnO_2 NWs with Sn nanoclusters with the spacing between them accommodating the 259% volume expansion of Sn when it forms Li–Sn alloys. The Sn-nanocluster-covered SnO_2 NWs have been shown to sustain

the mechanical stability of the material for up to 100 cycles with reversible capacity retention of over 800 mAh g^{-1} [23]. The columbic efficiency is over 98% and the capacity fading is low compared with other nanoscale SnO_2 material systems. This concept demonstrates how many metal oxide systems could be used to prevent chemical degradation while retaining high capacity. Other studies involving NWs of Co_3O_4 suggest similar phenomena [24–26].

In terms of illustrating efficient charge transport in NW-based systems, MoO_3 NW arrays grown on steel substrates shown in figure 4(*b*) are tested for lithium intercalation properties. The first cycle performance of molybdenum oxide (MoO_3) NPs and NWs is compared in figure 4(*c*). The data show an evident difference in the specific capacity during the first cycle with the NWs retaining 120 mAh g^{-1} higher capacity than the NPs. These results are discussed in detail elsewhere [27]. The data shown in figure 4(*c*). The enhanced performance with capacity retention is attributed to better conductivity in NW arrays compared with nanoparticulate thin films.

For cathode materials, there has been limited progress in the use of NW-based materials due to more emphasis on finding a suitable material with high capacity and potential. $Li_xMn_{0.67}Ni_{0.33}O_2$ NWs show capacity retention of 240 mAh g^{-1} for 12 cycles at a rate of 20 mA g^{-1} with good mechanical integrity [28]. Similarly, $Li_{0.88}[Li_{0.18}Co_{0.33}Mn_{0.49}]O_2$ NWs with a layered architecture show a high capacity retention of 220 mAh g^{-1} at 15 C rate [29]. Hence, NWs show tremendous promise as potential candidates for both electrode types in lithium-ion batteries.

Electrochromic devices change their optical properties when an electric potential is applied to them. The performance of these devices largely depends on the film composition, morphology and phase of the material. Nanocrystalline forms of electrochromic materials offer higher porosity while still maintaining the high intercrystalline contact necessary for electrical conductivity. Such films have higher transmission and are expected to exhibit better electrochromic optical modulation compared with the conventional films due to their open structure. However, transport of ions and electrons inside a nanocrystalline network is slow because of the presence of grain boundaries, causing the switching speeds to be long. NWs provide faster conduction pathways and thus faster switching in these types of devices.

It was shown that electrochromic devices made with vertical arrays of NWs of diameters in the range 40–60 nm possess high transmission modulation of about 50% at 700 nm [30]. The coloration process follows a biexponential function with time constants of 38 and 1.2 s while bleaching follows a single time constant of 138 s. The two time constants observed during coloration were attributed to diameter distribution in these NWs. Faster time constants were observed from the rapid coloration of the 40–60 nm diameter NWs while the slower time constants were observed from bundled NWs. These values are consistent with the time constants obtained theoretically, assuming a diffusion constant of 10^{-11} cm^2 s^{-1} for Li^+ ion inside WO_3 solid [31]. The characteristic time scales were estimated from the expression $\tau = l^2/D$, where l is the 'diameter' of the NW and D is the diffusion constant of Li^+ ions in WO_3. In NWs, there are typically two characteristic dimensions, i.e. diameter and length. The majority of the intercalation and deintercalation in NWs occurs through the walls of the NWs. Therefore, the characteristic length in these structures for the intercalation and deintercalation is the diameter of the wires. Using this expression, the time constant for individual and bundled NWs was 2.5 and 90 s, respectively. The bleaching process in these films was very slow. The time constant for bleaching in the vertically oriented NWs was 138 s. This can be attributed to the slower rates of deintercalation from the bundles and thick wires [32]. The deintercalation from the thin NWs does not seem to affect the optical contrast in the films. The slow bleaching is characteristic of the continued bleaching taking place from the thick 300 nm NWs. In addition to this process, the intercalation and deintercalation kinetics are also affected by the Li^+ ion concentration in the films.

4. Creation of new materials using NWs

In many material systems, it is difficult to synthesize epitaxial layers of single crystals of materials with low defect densities. Synthesis of relatively defect free NWs with lengths exceeding micrometres has been reported for various material systems such as GaN [33], GaAs [34] and InP [35]. However, for many material systems, the synthesis methods for NWs are not easy and straightforward without the use of catalysts. Below, we show two strategies in which NWs could be transformed from one type of material to another (oxides to nitrides or sulfides, etc) or be used as substrates for heteroepitaxial growth of materials with large lattice mismatching.

4.1. Phase transformation of NWs

It is very easy to synthesize NWs of oxides for a variety of material systems. To expand the utility of the synthesis techniques developed for oxides, one needs to explore ways of transforming oxides into other compositions. Not a great deal of research has been done on phase transformation of 1D nanostructures. Recently, we showed that it is easy to transform oxides to nitrides and sulfides without compromising single crystallinity [36]. In the case of NWs, the diameter is on the order of nanometre scale, which is on the order of reaction diffusion length scale for many species, as shown in figure 5(*a*). For thin films, complete phase transformation is difficult, as the diffusion of species into and out of the film limits the rate of transformation with increasing thickness and also results in polycrystallinity due to random nucleation.

Hematite shows a great deal of promise in photoelectrochemical water splitting, but pyrite, FeS_2, has also gained support as an earth abundant material for photovoltaics. In this regard, FeS_2 phase NWs are of significant interest to photovoltaic applications. Here, we show a simple procedure of converting hematite NWs using sulfurization reaction. As shown in the next section, hematite (Fe_2O_3) NWs can also be formed easily by rapid exposure of iron foil to oxygen plasma. The α-Fe_2O_3 NW arrays grown on iron foils were placed on a boron nitride heater in a small vacuum chamber, with 25 sccm

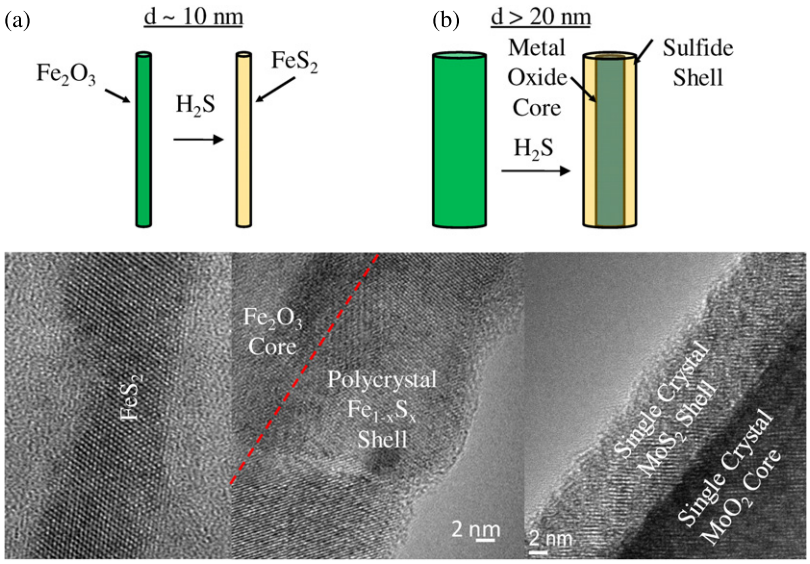

Figure 5. Phase transformation and/or modification of NWs using gas phase reaction: (*a*) schematic illustrating possible single crystal to single crystal transformation using gas phase reactions when diameters are less than 10 nm, (*b*) schematic illustrating diffusional limitation for sulfurization reaction forming core–shell structure when diameters are greater than 20 nm, (*c*) HRTEM image of a single crystal FeS_2 resulting with sulfurization of sub-10 nm diameter Fe_2O_3 NW, (*d*) HRTEM image of a-Fe_2O_3 core with polycrystalline $Fe_{1-x}S_x$ shell formed with sulfurization of thick Fe_2O_3 NW and (*e*) HRTEM image showing single crystal MoS_2 shell on MoO_2 core with sulfurization of thick MoO_3 NW.

of H_2S. The sample was heated to approximately 250 °C at a chamber pressure of 80 mTorr and the sulfurization was conducted for 1 h. The results suggest that the sulfurization of NWs appears to be diameter dependent as indicated in schematics in figures 5(*a*) and (*b*). For oxide NWs with diameters around 10 nm, complete conversion to single crystal FeS_2 can be observed (figure 5(*c*)). Larger diameter wires, on the order from 20 to 100 nm, show a polycrystalline shell morphology, as shown in figure 5(*d*). This sulfide shell is a non-stoichiometric $Fe_{1-x}S_x$; the polycrystalline shell can be due to both diffusion limits of S atoms through the metal sulfide and large mismatching of lattice parameters. A very long annealing time at higher temperatures may increase the thickness of the shell, but temperatures must be kept relatively low to prevent decomposition. Sulfur atoms diffuse into the lattice converting the oxide to sulfide with release of oxygen atoms. Subsequent conversion is hampered by the FeS_2 shell that has a very small diffusion coefficient for S atoms, which explains the observed maxima in the shell diameter. The ability to attain single crystalline pure phase FeS_2 NWs is entirely due to the available surface for the diffusion of S atoms, which is not possible in the case of thin films.

MoS_2 is a potential material for photoelectrochemical water splitting, but synthesis of the material in NW format can be a challenge. Single crystalline MoO_3 NWs with diameters of 20–50 nm and 1–2 μm lengths have been synthesized via hot filament chemical vapour deposition (HFCVD) on FTO substrates. The synthesized NWs were annealed in a H_2S atmosphere at relatively low temperatures (<200 °C) for conversion from oxide to sulfide. Even after longer reaction times, the diffusion limits of S atoms through the MoS_2 shell prevents complete conversion of the NWs with thicknesses greater than 20 nm. Such diffusion limitations have been seen in other NW systems [37]. A single crystal MoS_2 shell forms outside of a single crystalline MoO_2 core, which can be seen in figure 5(*e*).

4.2. Creation of new materials using heteroepitaxy on NWs

NWs can also be used as substrates for heteroepitaxial growth of single crystalline layers of materials that otherwise could not be obtained. Here, we show an important example with synthesizing single crystalline layers of ternary III-nitride materials of various compositions. Ternary III–V materials are very promising for a variety of opto-electronic [38–42] and energy conversion applications [43, 44] due to their tunable composition-dependent band gap. In the case of InGaN, the band gap of the alloy can be tuned from 0.8 to 3.4 eV by varying the composition of the alloy, which opens up numerous applications. The caveat here is that the atomic sizes of the constituent materials are so different that the alloy has a lot of built-in stress due to the composition. However, with the lack of native epitaxial substrates, lattice mismatched substrates are used to grow the alloys that induce huge composition- and thickness-dependent stresses in the film. Applications such as solar cells and photoelectrochemical water splitting require mid- to high indium composition alloys that result in a lot of stress leading to phase segregation and the formation of dislocations, which damages the material quality and performance.

There have been some reports on the synthesis of InGaN alloys, but they have either been very thin films (inefficient light absorbers) [39], low indium content alloys (large band gap) [45] or all the compositions were grown on one substrate (lack of control over alloy composition) [46]. Indeed, the composition-controlled synthesis of InGaN NWs with high indium content still remains a challenge. The planar substrates tend to be rigid whereas NWs can act as semi-rigid

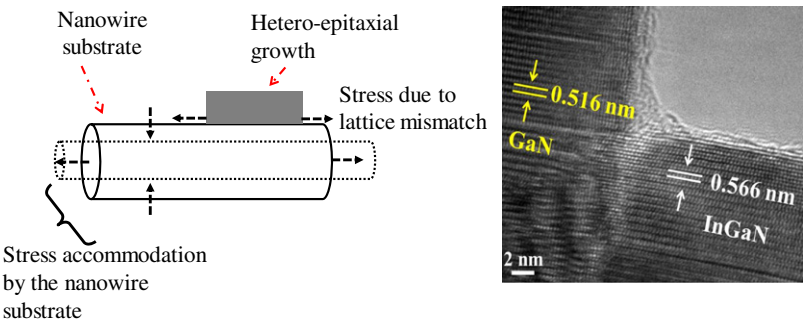

Figure 6. The use of NWs as substrates for growing epilayers of materials with large lattice mismatching: (*a*) schematic illustrating various modes of strain relaxation during epitaxial growth on a NW substrate; (*b*) HRTEM image showing epitaxial growth of InGaN on GaN NW substrate.

substrates owing to the small diameters wherein the lattice can deform and thus accommodate a part of the stress. This is illustrated in figure 6(*a*). The stress accommodation by the NW is then translated into reduced stress on the alloy, allowing for a stable single crystalline growth without phase segregation. Figure 6(*b*) is the high-resolution transmission electron microscopy (HRTEM) image of InGaN growth on GaN NWs where epitaxial and dislocation-free growth is clearly evident. Lattice spacing can be correlated with the alloy composition where GaN NW lattice can be used as an internal calibration. Detailed discussion on the nature and mechanism of InGaN alloy growth is available elsewhere [47]. Also, it has been shown that the composition of InGaN alloys can be controlled using heteroepitaxial growth on pre-synthesized GaN NWs with diameters in the 15–25 nm range as substrates [47].

5. A scalable plasma-based process for NW arrays

NWs have been synthesized using a variety of techniques, including both gas-phase- and liquid-phase-based methods [48]. Most of the known methods can only synthesize NWs in milligram amounts over long time durations (hours or days) and thus are not suitable for commercialization. NW arrays have been synthesized onto a variety of substrates using methods such as thermal oxidation [49, 50], plasma exposure of foils [51–53], HFCVD [54] and Si NWs on different templates [20]. Large-scale production of NWs is even more difficult and only few methods can potentially synthesize NWs in appreciable quantities. These methods include the HFCVD [54], super critical fluid [55], hydrothermal [56], flame synthesis [57], fluidized bed [58] and plasma foil or substrate oxidation [59, 60] approaches. Of these methods, gas phase synthesis using microwave plasma is the fastest and most suitable for commercialization because of the large-scale production potential.

Here, a scalable plasma-based process for direct gas phase synthesis of NW arrays directly over their respective metal foil is discussed. This direct gas phase method employs microwave plasma discharge (at 2.45 GHz), which is suitable for generating a highly dense, large volume plasma without any electrodes (as in dc plasma discharge) or co-axial cables (as in RF plasma discharge). The low power loss and ability to rapidly synthesize the desired material because of the presence of highly reactive ions, atoms, molecules and other active species makes it an ideal solution for high-throughput roll-to-roll manufacturing of NW arrays directly onto metal rolls. Figure 7 depicts the scheme for roll-to-roll manufacturing of iron oxide NWs arrays over iron foils as an example. Each spot (of area 1 × 1 inch^2) on the iron foil roll can be exposed to the overhead microwave plasma discharge for about 2 min. The final product will be vertical arrays of iron oxide NW arrays emanating perpendicularly to the surface of the entire foil. Since the substrate is a firm conducting surface, such architecture can be used directly for a variety of applications.

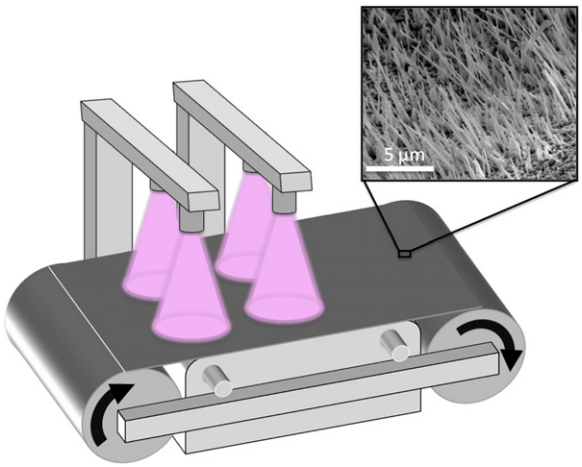

Figure 7. Schematic illustrating 'roll-to-roll' manufacturing scalability of our growth process, i.e. rapid and direct oxidation of metal foils using atmospheric plasmas for metal oxide NW arrays. The inset shows synthesis of copper oxide NW arrays grown directly on copper foils.

A batch plasma oxidation procedure involving an iron foil (of area 1 × 1 cm^2) took about 2 min to synthesize iron oxide NW arrays. The reactor details for metal foil oxidation are described elsewhere [60–62]. Briefly, the oxidation experiments were conducted in a microwave plasma reactor operating at atmospheric pressures. The batch operation involved exposing a clean iron foil vertically over a plasma flame at 1 kW power sustained with 11 slpm air for about 2 min. This resulted in vertical arrays of iron oxide NWs across the entire exposed surface of the foil. The colour of the iron foil becomes rusty, which is a characteristic of iron oxide NW

formation. The resulting NWs are wider at the base (about 100 nm wide) and become narrower towards the tip. The NW length is about 5 μm.

The NW growth occurs by a vapour–solid–solid (VSS) growth mechanism where gas species diffuse and react at the solid surface and form a solid oxide layer, which serves as the source of NW growth. First, upon plasma exposure, oxygen radicals recombine onto the iron foil (exothermic reaction) and heat up the foil surface thus creating an iron oxide layer. Further dissolution of gas phase species leads to super saturation followed by spontaneous formation of Fe_2O_3 nuclei, which occurs at a foil temperature of about 580 °C based on the Fe–O phase diagram [49, 63–65]. Further diffusion of O or O_2 radicals/atoms/molecules through the oxide layer coupled with the low mobility of iron at the synthesis temperature results in the vertical arrays of NWs above the oxide layer.

The NW growth occurs at temperatures lower than the melting temperatures of the respective metal foil. It must be noted that a delicate temperature (or plasma power) of the foil surface is essential for the desired NW array formation. Too low temperature or plasma power leads to the formation of flakes, which grow laterally onto the surface, while high temperature or high plasma power leads to the formation of a flat oxide layer. It is observed that flakes can be converted to NW arrays by exposing them to slightly denser plasma at comparatively higher temperatures. The flat oxide layer is due to increased mobility of iron and random diffusion at higher temperatures.

The advantages of this scheme outweigh its disadvantages. Unlike low-pressure plasma exposure reactors, the open nature of flame and atmospheric pressure exposure renders this scheme very simple for commercial roll-to-roll manufacturing. There is no need for any vacuum components and there is freedom in terms of modifying components to the reactor without having to confine them to a low-pressure environment. However, one disadvantage is that the temperature fluctuations can sometimes lead to undesired product, as this process is highly sensitive to the foil temperature.

6. Concluding remarks

NWs with diameters on the order of 10–100 nm range are interesting for a variety of electrochemical and photoelectrochemical energy conversion and storage applications due to enhanced charge transport properties and reduced length scales for charge transport and intercalation. NWs with smaller diameters are also interesting for creating new materials with well-defined crystallinity and compositional control that are otherwise difficult to synthesize. The practical implication of NW-based materials toward energy conversion and storage applications will rely primarily on the development of scalable and cost effective nanomanufacturing techniques for NW arrays over large areas and bulk quantities of NW powders. A simple procedure of utilizing an atmospheric plasma for creating hematite NW arrays on iron foils is shown and is also illustrated with a schematic on how this technique could be implemented as a roll-to-roll processing technique.

Acknowledgments

Authors acknowledge the financial support from the US Department of Energy (DE-FG02-07ER46375 and 10EE0003206), fellowship support to H B Russell from the Kentucky Space Grant Consortium, financial support from the Kentucky Renewable Energy Consortium (KREC), and the contributions of several former students from this research group (Dr Suresh Gubbala and Boris Chernomordik) and current collaborators (Professor Gamini Sumanasekera at UofL and Dr Miran Mozetic and Dr Uros Cvelbar at Institute Jozef Stefan) for technical discussions in the last several years. The authors thank Andrew Marsh at the Conn Center for Renewable Energy Research for technical editing services.

References

[1] Brus L 1986 *J. Phys. Chem.* **90** 2555
[2] Yu H, Li J, Loomis R A, Wang L W and Buhro W E 2003 *Nature Mater.* **2** 517
[3] Yang P, Yan R and Fardy M 2010 *Nano Lett.* **10** 1529
[4] Bak T, Nowotny J, Rekas M and Sorrell C C 2002 *Int. J. Hydrogen Energy* **27** 991
[5] Vayssieres L, Sathe C, Butorin S, Shuh D, Nordgren J and Guo J 2005 *Adv. Mater.* **17** 2320
[6a] Itoh K and Bockris J O 1984 *J. Electrochem. Soc.* **131** 1266–71
[6b] Rosso K M, Smith D M A and Dupuis M 2003 *J. Chem. Phys.* **118** 6455
[7] Ahmed S M, Leduc J and Haller S F 1988 *J. Phys. Chem.* **92** 6655
[8] Cesar I, Sivula K, Kay A, Zboril R and Graetzel M 2009 *J. Phys. Chem. C* **113** 772
[9] Chernomordik B, Russell H B, Cvelbar U, Jasinski J B, Kumar V, Deutsch T and Sunkara M K 2010 submitted
[10] Regan O and Gratzel M 1991 *Nature* **353** 737
[11] Fessenden R W and Kamat P V 1995 *J. Phys. Chem.* **99** 12902
[12] Tachibana Y, Moser J E, Gratzel M, Klug D R and Durrant J R 1996 *J. Phys. Chem.* **100** 20056
[13] Hilgendorff M and Sundstrom V 1998 *J. Phys. Chem.* B **102** 10505
[14] Van de Lagemaat J, Park N-G and Frank A J 2000 *J. Phys. Chem.* B **104** 2044
[15] Tetreault N *et al* 2010 *ACS Nano* **4** 7644–50
[16] Gubbala S, Russell H B, Shah H, Deb B, Jasinski J, Rypkema H and Sunkara M K 2009 *Energy Environ. Sci.* **2** 1302
[17] Gubbala S, Chakrapani V, Kumar V and Sunkara M K 2008 *Adv. Funct. Mater.* **18** 2411
[18] Bruce P G, Scrosati B and Tarascon J M 2008 *Angew. Chem. Int. Edn Engl* **47** 2930
[19] Aric A S, Bruce B, Scrosati B, Tarascon J M and Schalkwijk W V 2005 *Nature Mater.* **4** 366
[20] Chan C K, Peng H, Liu G, McIlwrath K, Zhang X F, Huggins R A and Cui Y 2008 *Nature Nanotechnol* **3** 31
[21] Chan C K, Zhang X F and Cui Y 2008 *Nano Lett.* **8** 307
[22] Lee H and Cho J 2007 *Nano Lett.* **7** 2638
[23] Meduri P, Pendyala C, Kumar V, Sumanasekera G U and Sunkara M K 2009 *Nano Lett.* **9** 612
[24] Poizot P, Laruelle S, Grugeon S, Dupont L and Tarascon J M 2008 *Nature* **2000** 407
[25] Nam K T, Kim D-W, Yoo P J, Chiang C-Y, Meethong N, Hammond P T, Chiang Y-T and Belcher A M 2006 *Nature* **312** 885
[26] Li Y, Tan B and Wu Y J 2008 *Nano Lett.* **8** 265
[27] Meduri P, Clark E, Dayalan E, Sumanasekera G U and Sunkara M K, in preparation

[28] Park D H, Lim S T, Hwang S J, Yoon C S, Sun Y K and Choy J H 2005 *Adv. Mater.* **17** 2834
[29] Lee Y, Kim M G and Cho J 2008 *Nano Lett.* **8** 957
[30] Gubbala S, Thangala J and Sunkara M K 2007 *Sol. Energy Mater. Sol. Cells* **91** 813
[31] Granqvist C G 2000 *Sol. Energy Mater Sol. Cells* **60** 201
[32] Gubbala S 2009 *PhD Dissertation* University of Louisville
[33] Bertness K A, Roshko A, Mansfield L M, Harvey T E and Sanford N A 2008 *J. Cryst. Growth* **310** 3154
[34] Wacaser B A, Deppert K, Karlsson L S, Samuelson L and Seifert W 2006 *J. Cryst. Growth* **287** 504
[35] Krishnamachari U, Borgstrom M, Ohlsson B J, Panev N, Samuelson L, Seifert W, Larsson M W and Wallenberg L R 2004 *Appl. Phys. Lett.* **85** 2077
[36] Thangala J, Chen Z Q, Chin A H, Ning C Z and Sunkara M K 2009 *Cryst. Growth Des.* **9** 3177
[37] Dloczik L and Konenkamp R 2003 *Nano Lett.* **3** 651
[38] Kung P and Razeghi M 2000 *Opto-Electron.* **8** 201
[39] Qian F, Gradeak S, Li Y, Wen C-Y and Lieber C M 2005 *Nano Lett.* **5** 2287
[40] Nakamura S 1997 *Solid State Commun.* **102** 237
[41] Nakamura S 1999 *Semicond. Sci. Technol.* **14** R27
[42] Tamboli1 A C, Haberer E D, Sharma R, Lee K H, Nakamura S and Hu E L 2007 *Nature Photon.* **61** 61–4
[43] Wu J, Walukiewicz W, Yu K M, Shan W, Ager III J W, Haller E E, Lu H, Schaff W J, Metzger W K and Kurtz S 2003 *J. Appl. Phys.* **94** 6477
[44] Li J, Lin J Y and Jiang H X 2008 *Appl. Phys. Lett.* **93** 162107
[45] Kim H-M, Lee H, Kim S I, Ryu S R, Kang T W and Chung K S 2004 *Phys. Status Solidi* **241** 2802
[46] Kuykendall T, Ulrich P, Aloni S and Yang P 2007 *Nature Mater.* **6** 951
[47] Pendyala C, Kim J H, Jasinski J B and Sunkara M K 2010 submitted
[48] Meyyappan M and Sunkara M K 2009 *Inorganic Nanowires: Applications, Properties and Characterization* (Boca Raton, FL: CRC Press)
[49] Wen X, Wang S, Ding Y, Wang Z L and Yang S 2005 *J. Phys. Chem.* B **109** 215
[50] Ghoshal T, Biswas S, Kar S, Dev A, Chakrabarti S and Chaudhuri S 2008 *Nanotechnology* **19** 065606
[51] Mozetic M, Cvelbar U, Sunkara M K and Vaddiraju S 2005 *Adv. Mater.* **17** 2138
[52] Cvelbar U, Chen Z, Sunkara M K and Mozetic M 2008 *Small* **4** 1610
[53] Chen Z Q, Cvelbar U, Mozetic M, He J Q and Sunkara M K 2008 *Chem. Mater.* **20** 3224
[54] Thangala J, Vaddiraju S, Bogale R, Thurman R, Powers T, Deb B and Sunkara M K 2007 *Small* **3** 890
[55] Yu D P, Xing Y J, Hang Q L, Yan H F, Xu J, Xi Z H and Feng S Q 2001 *Physica* E **9** 305
[56] Holmes J D, Johnston K P, Doty R C and Korgel B A 2000 *Science* **287** 1471
[57] Zhang Y X, Li G H, Jin Y X, Zhang Y, Zhang J and Zhang L D 2002 *Chem. Phys. Lett.* **365** 300
[58] Athanassiou E K, Grossmann P, Grass R N and Stark W J 2007 *Nanotechnology* **18** 165606
[59] Glushenkov A M, Stukachev V I, Hassan M F, Kuvshinov G G, Liu H K and Chen Y 2008 *Cryst. Growth Des.* **8** 3661
[60] Kumar V, Kim J H, Pendyala C, Chernomordik B and Sunkara M K 2008 *J. Phys. Chem.* C **112** 17750
[61] Kim J H, Kumar V and Sunkara M K 2008 *Midem* **38** 237
[62] Kumar V, Kim J H, Jasinski J, Clark E L and Sunkara M K 2010 submitted
[63] Cvelbar U and Ostrikov K 2008 *Cryst. Growth Des.* **8** 4347
[64] Ostrikov K, Levchenko I, Cvelbar U, Sunkara M K and Mozetic M 2010 *Nanoscale* **2** 2012
[65] Cvelbar U, Ostrikov K, Levchenko I, Mozetic M and Sunkara M K 2009 *Appl. phys. lett.* **94** 211502